

Binary Poly(ethylene oxide)/Poly(methyl methacrylate-*co*-ethyl methacrylate) Blends: Miscibility Predictions from Model Compound Mixtures vs Experimental Phase Behavior

J. A. Pomposo,[†] R. de Juana, A. Múgica, and M. Cortázar*

Departamento de Ciencia y Tecnología de Polímeros, Facultad de Ciencias Químicas de San Sebastián, P.O. Box 1072, E-20080 San Sebastián, Spain

M. A. Gómez

Instituto de Ciencia y Tecnología de Polímeros, Juan de la Cierva 3, E-28006 Madrid, Spain

Received December 26, 1995; Revised Manuscript Received July 8, 1996[®]

ABSTRACT: Employing segmental interaction densities (B_{ij} 's) determined by means of analogue calorimetry, a binary interaction model based on the Flory–Huggins theory predicts the miscibility of poly(ethylene oxide) (PEO) with poly(methyl methacrylate-*co*-ethyl methacrylate) [P(MMA-*co*-EMA)] copolymers having high methyl methacrylate contents. The miscibility behavior of PEO with P(MMA-*co*-EMA) containing 60 wt % methyl methacrylate was investigated in blends prepared by four different mixing methods. The miscibility in the amorphous state was studied by differential scanning calorimetry (DSC), dynamic-mechanical thermal analysis (DMTA), and solid-state ^{13}C NMR spectroscopy techniques. Glass transition (T_g) and α -relaxation (T_α) results shown miscibility for blends with PEO content lower than 20 wt %. Blends with PEO content higher than 20–40 wt % show both T_g and T_α values very similar to those of pure PEO. The presence of a second amorphous phase composed of PEO and the copolymer could only be detected by DMTA. The intimacy of mixing in this amorphous phase was supported by ^{13}C NMR. The melting and crystallization behavior was also investigated. The small depression in the experimental melting temperatures did not allow a definite conclusion about the homogeneity of this system in the molten state to be obtained. The addition of the copolymer did not have a great influence on the spherulite growth rate of PEO, this behavior being that expected of a multiphasic blend. Moreover, a new analysis proposed in this paper was able to explain the crystallization behavior of these blends, assuming that diffusion takes place from an immiscible melt. These results are in good agreement with the miscibility predictions from model compound mixtures.

Introduction

Copolymer blend miscibility has been well-studied in recent years, although much work must still be done to understand the complex balance of interactions involved. Among other factors,^{1,2} the phase behavior of a copolymer blend depends on the inter- and intramolecular interactions, the molecular weight of the components, and the differences in conformation and chain flexibility of the polymer chains.

Further complexity is introduced when a crystallizable component is present,^{2–4} since the crystallization phenomena normally make the determination of blend miscibility a difficult task. To alleviate this problem, several approaches can be adopted. On the one hand, experimental techniques of increasing resolution power can be combined to establish the degree of homogeneity of the blends in the amorphous phase. On the other, specific treatments may be used to reduce blend crystallinity and, hence, to increase the total amount of amorphous material in the system. Finally, different blend preparation methods could be employed to ascertain the influence of the mixing procedures on blend miscibility. An indication of blend compatibility in the molten state can be also obtained by a proper analysis of the melting and crystallization behavior of the system.

Concerning the molecular origin of copolymer blend miscibility, significant insight has been achieved since

the introduction of the simple binary interaction model.^{5–7} The concept of repulsive interactions^{8–10} between monomer units in some copolymers improving blend miscibility is widely accepted. According to the following expression, the blend interaction energy density, B , for mixing a random copolymer $\text{C}_x\text{D}_{(1-x)}$ and a homopolymer A is:

$$B = xB_{AC} + (1 - x)B_{AD} - x(1 - x)B_{CD} \quad (1)$$

where B_{ij} is the interaction energy density of each pair of polymer repeat units involved, and x is the volume fraction of C units in the copolymer. In addition to this theoretical framework, a number of studies^{11–14} have been devoted to illustrate how the enthalpy of mixing results from low molecular weight analogue liquids can provide guidance to the polymer blend miscibility. As a rule, good first-order, enthalpy-based estimates of the interaction energy densities of polymer blends can be obtained from analogue calorimetry, even when this approximation fails to capture several other inherent factors affecting the miscibility of macromolecules.

The purpose of this work is to examine the miscibility pattern of blends of poly(ethylene oxide) (PEO), a typical crystalline homopolymer, and poly(methyl methacrylate-*co*-ethyl methacrylate) [P(MMA-*co*-EMA)], the selected amorphous copolymer. It is well-known that blends of PEO and atactic poly(methyl methacrylate) (PMMA) are miscible. The interaction parameter obtained for this system from melting point depression studies^{15–18} and by small angle neutron scattering¹⁹ is negative, although very small in absolute magnitude. Martuscelli et al. have suggested from melting point

* Author to whom correspondence should be addressed.

[†] Present address: SAIOLAN, P.O. Box 23, E-20500 Mondragón, Spain.

[®] Abstract published in *Advance ACS Abstracts*, September 15, 1996.

studies that poly(ethylene oxide)/poly(ethyl methacrylate) (PEMA) blends are miscible in the molten state.^{20,21} Furthermore, as reported by several authors, the two methacrylate polymers PMMA and PEMA are immiscible with each other.^{22–24} Consequently, the three independent binary interaction parameters involved in eq 1 should result in a negative interaction parameter between the PEO homopolymer and P(MMA-co-EMA) copolymers, and hence, the resulting system should be miscible. In the framework of the binary interaction theory, the addition of PEO to the copolymer will result in a dilution of the unfavorable interactions between methyl methacrylate (MMA) and ethyl methacrylate (EMA) segments, leading to a net exothermic B parameter.

In this paper we employed the analogue calorimetry approach in order to model the different interactions in PEO/P(MMA-co-EMA) blends, by using low molecular weight liquids with structures resembling those of the polymers. The miscibility predictions of the binary interaction model were then experimentally checked by employing a variety of techniques with gradual resolution power ranging from microscopic and thermal analysis to spectroscopic techniques. Furthermore, the crystallization behavior of the blends was analyzed in terms of recent theories incorporating diffusional concepts in the description of the secondary crystallization process. Finally, several subtle effects which could modify the miscibility behavior of the PEO/P(MMA-co-EMA) system are pointed out.

Experimental Section

Materials. Poly(ethylene oxide) and poly(methyl methacrylate-co-ethyl methacrylate) containing 60% methyl methacrylate by weight were supplied by Polysciences. The molecular weights determined by gel permeation chromatography (GPC) in tetrahydrofuran were $M_n = 41\,000$, $M_w = 78\,000$ for PEO and $M_n = 177\,000$, $M_w = 473\,000$ for the copolymer. The copolymer composition was verified by ^1H NMR. The ratio of isotactic (mm) to heterotactic (mr or rm) to syndiotactic (rr) triads in the copolymer was obtained from the signal C_α of the typical ^{13}C NMR. The ratio was about 5/36/59 that expected if the generation of configurational sequences follows Bernoullian statistic²⁵ with a probability of meso placement (Pm) equal to 0.22. The copolymer and the PEO were purified by dissolving in chloroform and precipitating the resulting solutions with vigorous stirring into a large excess of cold methanol or hexane, respectively. This procedure was repeated twice and the precipitated polymers were dried in a vacuum oven at 50 °C until constant weight was obtained from repeated measurements.

Methyl isobutyrate (MIB) and ethyl isobutyrate (EIB) were employed as low molecular weight analogues of the repeat units comprising the P(MMA-co-EMA) copolymer. Tetraethylene glycol dimethyl ether (TEGDME) was assumed to closely resemble the PEO chemical structure and therefore was used as the model compound for this polymer. These materials were obtained from Aldrich (99% pure) and used as received without further purification.

Blend Sample Preparation. Since blending conditions could play an important role in miscibility studies, different mixing techniques were employed in the preparation of the polymer blends. Firstly, films were obtained by dissolving the two components in the desired proportions in chloroform at a 2% w/v concentration, followed by casting of the resulting solutions in glass dishes. The solvent was then allowed to evaporate slowly in air at room temperature. Secondly, freeze-dried samples were prepared by mixing the pure polymers in the appropriate proportions in benzene (2% w/v). After freezing the solution into liquid nitrogen, the benzene was sublimed from the polymer samples using a vacuum pump. Blends were also prepared by the solution-precipitation procedure. The

polymers were dissolved in chloroform and the solution was precipitated in *n*-hexane. All samples were further dried in a vacuum oven at 50 °C for 1 week.

The final method employed to prepare the samples was melt-mixing using a "Mini Max Molder" Model C. S. 183 MMX, equipped with a rotor control. The intimacy of mixing depends on the working conditions such as the temperature at which the sample is maintained, the residence time, and the rotor speed. After preliminary studies, optimal conditions were found to be 150–190 °C (depending on the composition of the blend), with a residence time of 13 min and a rotor speed of 100 rpm. This method, unlike the ones previously mentioned, has the advantage of not requiring the use of a solvent, which in some cases could modify the miscibility behavior of the system studied.

Analogue Calorimetry. Heats of mixing for low molecular weight analogues of the corresponding polymers were measured using a Setaram C80D flux-type calorimeter at 30.5 ± 0.1 °C. When necessary, premixes of model compounds were prepared in order to represent several copolymer compositions.

Differential Scanning Calorimetry (DSC). A Perkin-Elmer DSC-2C differential scanning calorimeter, equipped with a TADS microcomputer, was used to study the thermal behavior of the blends. The apparatus was routinely calibrated using indium and *n*-dodecane as standards.

Glass transition temperature (T_g) measurements were conducted by heating the samples from 150 to 420 K at 20 K/min and maintaining that temperature for 10 min before rapid quenching to 150 K. The samples were then reheated to 420 K and the T_g measured in this second scan for all samples, except for some samples where the T_g was also monitored in the first scan. Following the convention used in other thermal analysis techniques, in all cases the T_g was taken as the temperature at which the heat capacity reached one-half of the entire step change.

To obtain the melting temperatures (T_m) of samples crystallized isothermally at different temperatures (T_c), the samples were first melted at 373 K for 10 min to remove any previous traces of crystallinity. After cooling them quickly to T_c and keeping the samples at this temperature during the time necessary to reach a crystallization level of 50%, they were heated at a scanning rate of 10 K/min. The melting temperatures were taken as the onset of the corresponding melting peak.

Finally, the apparent enthalpies of melting were obtained from the melting peaks in a first run at a heating rate of 10 K/min.

Dynamic Mechanical Thermal Analysis (DMTA). Dynamic mechanical measurements were conducted on samples prepared by the casting method. These samples were moulded between two plates of a compression-moulding press at 100–140 °C, depending on the composition of the blend, and cooled at ambient temperature. A Polymer Laboratories dynamic mechanical thermal analyzer in the bending mode was used for dynamic mechanical testing over the temperature range from –100 °C until the sample became too soft to be further tested. The heating rate used was 4 °C/min, and the scans were performed at a frequency of 1 Hz.

Thermo-Optical Microscopy. The morphology and the isothermal growth rate (G) of PEO spherulites in freeze-dried blends were studied on thin films by using a Reichert polarizing optical microscope equipped with a Mettler PF5 hot stage. The films, sandwiched between a microscope slide and a cover glass, were first melted at 100 °C for 10 min in order, to eliminate any previous thermal history, and then rapidly cooled to the crystallization temperature. The size of growing spherulites was followed by taking photomicrographs at appropriate time intervals. The radial growth rate ($G = dR/dt$) was calculated from the lines obtained by plotting the average radius, R , of the spherulites against time, t .

Carbon-13 Solid-State NMR Spectroscopy. ^{13}C NMR spectra were recorded at ambient temperature on a Bruker MSL 400 spectrometer, operating at a static magnetic field strength of 9.3 T (^{13}C -resonance of 100.6 MHz). Magic angle spinning (MAS) of the samples was carried out with a Bruker MAS-DB7 double bearing probe head. A field strength of 50

Table 1. Model Compounds Used in This Study

compound	structure	density ^a (g/mL)	mol wt
TEGDME	CH ₃ O(CH ₂ CH ₂ O) ₄ CH ₃	1.009	222.3
MIB	(CH ₃) ₂ CHCOOCH ₃	0.891	102.1
EIB	(CH ₃) ₂ CHCOOCH ₂ CH ₃	0.869	116.2

^a At 298 K.

kHz was used for dipolar decoupling (DD). Aluminum oxide rotors with poly(chlorotrifluoroethylene) end caps containing 100 mg of sample were spun at speeds of *ca.* 4 kHz. The CH signal of adamantane (29.5 ppm downfield from tetramethylsilane) was used as the external reference.

The proton spin–lattice relaxation times in the rotating frame ($T_{1\rho}^H$) were obtained from plots of the decay of the relative magnitude of the carbon magnetization vs proton–carbon contact time in the usual cross polarization sequence.

Results and Discussion

Miscibility Predictions. As stated previously, the miscibility of PEO/P(MMA-*co*-EMA) blends is expected to be enhanced as a consequence of unfavorable interactions between the different repeat units comprising the P(MMA-*co*-EMA) copolymer.^{22–24} Such an effect can be quantified in terms of the binary interaction model summarized in eq 1, provided that the interaction energies between different repeat units are available or can be estimated. In this sense, analogue calorimetry has become a useful technique for obtaining rough estimates of polymer–polymer interaction energies from heat of mixing data of low molecular weight liquids having chemical structures closely related to those of the polymer repeat units.^{11–14} This approach was followed in this work, and the model compounds summarized in Table 1 were used. Premixes of EIB and MIB, which mimic the composition of P(MMA-*co*-EMA) copolymers, were prepared and the heats of mixing of such premixes and TEGDME were measured at 30.5 °C. The enthalpic interaction energy density (B_{ij}^h) was calculated from the heat of mixing ($\Delta H_m/V$) and the volume fraction of the two components (ϕ_k) as

$$B_{ij}^h = \frac{(\Delta H_m/V)}{\phi_i \phi_j} \quad (2)$$

Figure 1 shows the experimental B_{ij}^h parameters as a function of the volume fraction of EIB in the premix. The dashed line in this figure corresponds to the prediction from the binary interaction model (eq 1) in terms of the experimental interaction energies obtained in this work for TEGDME/MIB (−0.74 cal/mL), TEGDME/EIB (1.51 cal/mL), and MIB/EIB (0.49 cal/mL) mixtures. The good agreement between theoretical and experimental results lends support to the mean-field description of these mixtures, as embodied in eq 1.

The interaction energy between TEGDME and MIB obtained in this work compares favorably with that reported previously by Min et al.²⁶ (−0.9 cal/mL). Additionally, the well-known repulsive interaction in PMMA/PEMA blends²⁴ is also supported by the analogue calorimetry results obtained for MIB/EIB mixtures. The most striking feature, however, is the endothermic mixing of TEGDME with EIB, since Cimmino et al.²¹ have suggested that PEO and PEMA are miscible in the molten state. In this sense, the results in Figure 1 reveal that only P(MMA-*co*-EMA) copolymers with high methyl methacrylate content should be miscible with PEO. According to this simple analysis, the P(MMA-*co*-EMA) copolymer employed in this study

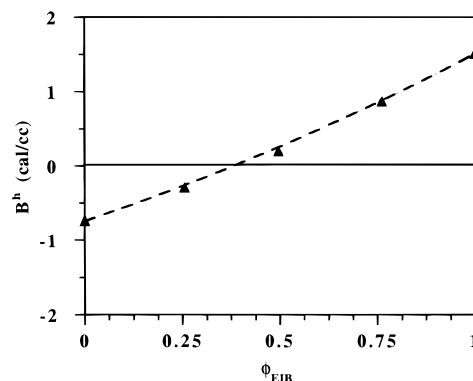


Figure 1. Enthalpic interaction energy density (B^h) as a function of the volume fraction of EIB in the MIB/EIB premix. The dashed line corresponds to the prediction from the binary interaction model (eq 1).

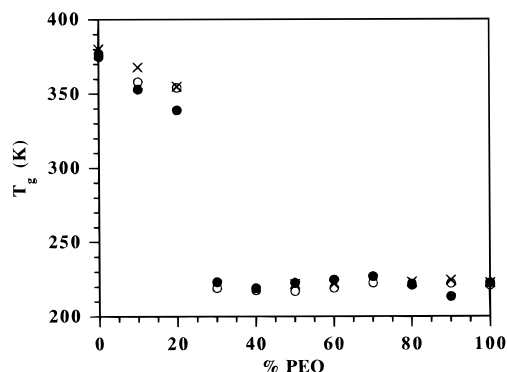


Figure 2. Composition dependence of the glass transition temperature (T_g) determined by DSC for PEO/P(MMA-*co*-EMA) blends as prepared by (●) melt-mixing, (○) solution-casting, and (×) freeze-drying.

having 60 wt % methyl methacrylate would be immiscible, or at least in the margin of miscibility, with PEO. Obviously, many other contributions affecting the miscibility of (co)polymer blends, such as free volume effects, nonrandom distribution of contacts due to chain connectivity and/or copolymer microstructure, and non-negligible entropic factors, could modify the present predictions extracted from heat of mixing data of model compounds.

Miscibility Behavior in the Amorphous Phase.

A generally accepted method to establish blend miscibility is the glass transition temperature (T_g) criterion. In a blend, the presence of a single T_g , which usually lies between those of the pure polymers, confirms the homogeneity of the system, i.e. the lack of phases with a diameter greater than about 150 Å.⁴ Conversely, a multiphase, immiscible blend will exhibit more than a single glass transition as a consequence of the different phases present in the system. In the limiting case of a totally immiscible binary blend, two T_g 's corresponding to the values of the pure components are expected across the entire composition range. Nevertheless, to ascertain the phase behavior of a blend, samples prepared by different methods should be studied.^{2,4}

Two experimental techniques, DSC and DMTA, were employed to study the T_g behavior. Referring to DSC, Figure 2 shows the T_g values determined from the second runs for PEO/P(MMA-*co*-EMA) samples prepared by different methods. As can be seen, there is good agreement between data obtained from different preparation procedures. In this figure, it is possible to distinguish two different behaviors. On one hand, P(MMA-*co*-EMA)-rich compositions (i.e. 90 and 80 wt

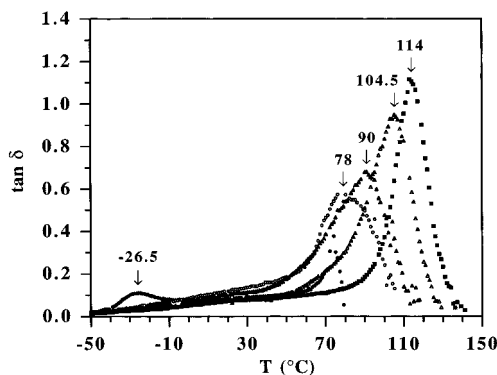


Figure 3. Dynamic mechanical spectra, at 1 Hz, for several copolymer-rich compositions of the PEO/P(MMA-co-EMA) system: (○) 40/60, (▲) 30/70, and (△) 10/90. Spectra of pure PEO (●) and pure P(MMA-co-EMA) (■) are also shown for comparison.

% copolymer) show a single glass transition which moves to lower temperatures as the percentage of PEO in the blend increases. According to the single T_g criterion, these compositions are miscible. On the other hand, samples containing 30 wt % or more PEO exhibit only one T_g , located near that of pure PEO, which does not change significantly with composition. In this case, it was not possible to verify the existence of a second T_g , although it could be hidden by the melting peak of PEO.

DMTA has the advantage over the calorimetric techniques that it is more sensitive² to smaller domain size and therefore it can reveal finer details.^{27,28} The dynamic mechanical spectra of the pure components and certain copolymer-rich blends are shown in Figure 3. The P(MMA-co-EMA) and PEO α -relaxations, regarded as the glass transition temperatures, are located at 114 and -26.5 °C, respectively. The spectrum corresponding to pure P(MMA-co-EMA) shows a prominent α -relaxation with a high $\tan \delta$ at the maximum, typical of amorphous polymers. In the dynamic mechanical spectrum of pure PEO, a peak at 74 °C was also detected, corresponding to the melting transition of PEO.

The copolymer-rich blends show a single α -relaxation lying between those of the pure components. Results for the sample PEO/P(MMA-co-EMA) 20/80 have been omitted in Figure 3 for clarity. The temperature and the relaxation intensity of these peaks change with blend composition, giving lower temperatures and smaller intensities as the amount of PEO in the blend increases. This behavior is normally accepted to be experimental evidence of miscibility. The observed broadening of the α -relaxation in the blends can be attributed to both local concentration fluctuations or to the overlapping of the melting peak of the semicrystalline phase of PEO with the α -relaxation of the blends. Unfortunately, the relatively small intensity of the β -relaxation of the P(MMA-co-EMA) copolymer as well as the peak broadening observed in the blends did not permit an estimation of the extent of mixing at the local scale of this secondary relaxation.^{29,30} Techniques with higher resolution power would be needed to determine the intimacy of mixing in these blends.

The loss tangent vs temperature plots for PEO-rich blends are illustrated in Figure 4. As has been stated before, the pure PEO presents a peak around -26.5 °C associated with the glass transition temperature. In the blends, the peak position does not shift significantly with composition, and for blends with copolymer content

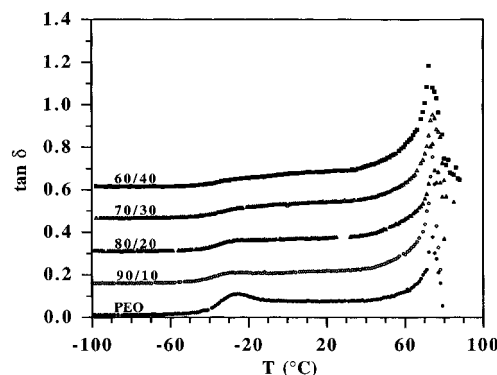


Figure 4. Dynamic mechanical spectra, at 1 Hz, for several PEO-rich compositions of the PEO/P(MMA-co-EMA) system: (●) 100/0, (○) 90/10, (▲) 80/20, (△) 70/30, and (■) 60/40.

higher than 40%, the α -relaxation of PEO cannot be clearly detected.

At this point, it is worth pointing out the complementary nature of DSC and DMTA. By DSC, lower amount of PEO (30 wt %) in the blend was required to detect an amorphous separate phase of pure PEO than that required by DMTA (60 wt %). Conversely, DMTA results show that there is a copolymer-rich phase having a clear T_g composition dependence (from 0 to 40 wt % PEO) which could not be detected by DSC at PEO contents higher than 20 wt %. Hence, although two amorphous phases are probably involved in most of the PEO/P(MMA-co-EMA) blends investigated, the DSC technique allows a better detection of the PEO-rich phase, whereas the copolymer-rich phase is more clearly detected by DMTA.

NMR relaxation times enable the phase behavior to be ascertained on a smaller scale than by T_g . Specifically, the spin-lattice relaxation time in the rotating frame, $T_{1\rho}^H$, represents an average value of the relaxation behavior over all protons in a polymer on a spatial scale around 30 Å.^{31,32} If two polymers are intimately mixed, the relaxation times of protons of different polymers should be equalized by spin-diffusion.³²⁻³⁴ Therefore, the $T_{1\rho}^H$ values for the blends will differ from those of the pure polymers and will change as a function of the mixture composition. When a polymer blend forms domains larger than approximately 30 Å, the $T_{1\rho}^H$ values are no longer averaged and the $T_{1\rho}^H$ values of the pure components will be obtained. Nevertheless, unexpected results have been found for polymer blends in which two phases of similar composition³⁵ or small discrete domains of one of the components^{36,37} are present. In addition, departures from the simple two-phase model above can be anticipated if interfacial effects take place (i.e. polymer mixing at the boundaries).

In this study, we performed high-resolution solid-state ^{13}C NMR measurements on PEO/P(MMA-co-EMA) blend samples prepared by freeze-drying. The assignments of the different peaks in the spectra of PEO and P(MMA-co-EMA) were made by reference to published data.³⁸ The $T_{1\rho}^H$ data were determined using the lines corresponding to the different carbons of the copolymer, and the values differed by no more than 10%. The carbon signal intensity decay curves were fitted to a standard first-order kinetic expression.³³ In Table 2 it can be observed that the experimental $T_{1\rho}^H$ values have a monotonic change with blend composition. The relaxation of P(MMA-co-EMA) in the blends compared with that in the pure state suggests that amorphous PEO

Table 2. $T_{1\rho}^H$ Relaxation Times (ms) of PEO/P(MMA-*co*-EMA) Blends at Room Temperature from P(MMA-*co*-EMA) Resonance Signals

PEO/P(MMA- <i>co</i> -EMA)	$T_{1\rho}^H$ (ms)
60/40	10.0
40/60	12.3
20/80	13.6
0/100	15.5

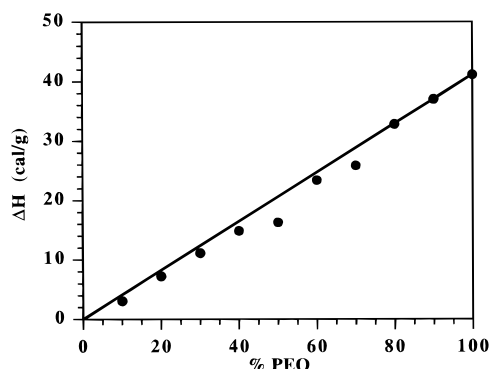


Figure 5. Composition dependence of the heat of fusion (ΔH) for PEO/P(MMA-*co*-EMA) blends prepared by the freeze-drying method as determined from the first DSC scan. The solid line gives the theoretical melting enthalpy of PEO in the pure state.

has mixed intimately with the copolymer to form a miscible phase. Apparently, this result could be in contradiction with the multiphasic nature of these blends observed by DSC and DMTA techniques. To discover if there were a second phase containing amorphous pure PEO, it would be necessary to observe how the ^{13}C signal corresponding to amorphous PEO is affected.

Although $T_{1\rho}^H$ values were also determined from observation of the PEO ^{13}C signal, our conclusions are based solely on the $T_{1\rho}^H$ relaxation behavior of the amorphous copolymer resonances in the blends, because the PEO signal resonance is, in fact, a composite of crystalline and amorphous peaks. We estimated the amount of crystalline PEO in the freeze-dried blends from first-scan DSC measurements by determining the heat of fusion per gram of blend (Figure 5). All blend compositions show values that fall close to the line which expresses the theoretical melting enthalpy of PEO as in the pure state. From Figure 5 we can conclude that these samples crystallize practically to the same extent as does pure PEO, and hence, a separate crystalline phase is present in these blends. Consequently, the $T_{1\rho}^H$ value of the PEO ^{13}C signal in the blend may have a significant contribution from the crystalline component, which undoubtedly would invalidate the analysis of blend miscibility in terms of this signal.

NMR experiments were carried out at room temperature with samples that had not suffered any previous heating. In light of the NMR results where the multifasic nature of the blends cannot be clearly shown, it is possible that the behavior obtained for PEO/P(MMA-*co*-EMA) blends in DSC and DMTA experiments could be a consequence of the thermal treatments given. In fact, it is well-known that most miscible polymer blends tend to phase separate at elevated temperatures.⁴ To verify if phase separation had taken place when these blends were heated in the DSC and DMTA experiments, particular attention was paid to the first DSC scans of the samples employed in the ^{13}C NMR experiments. Figure 6 presents the thermograms for the first and

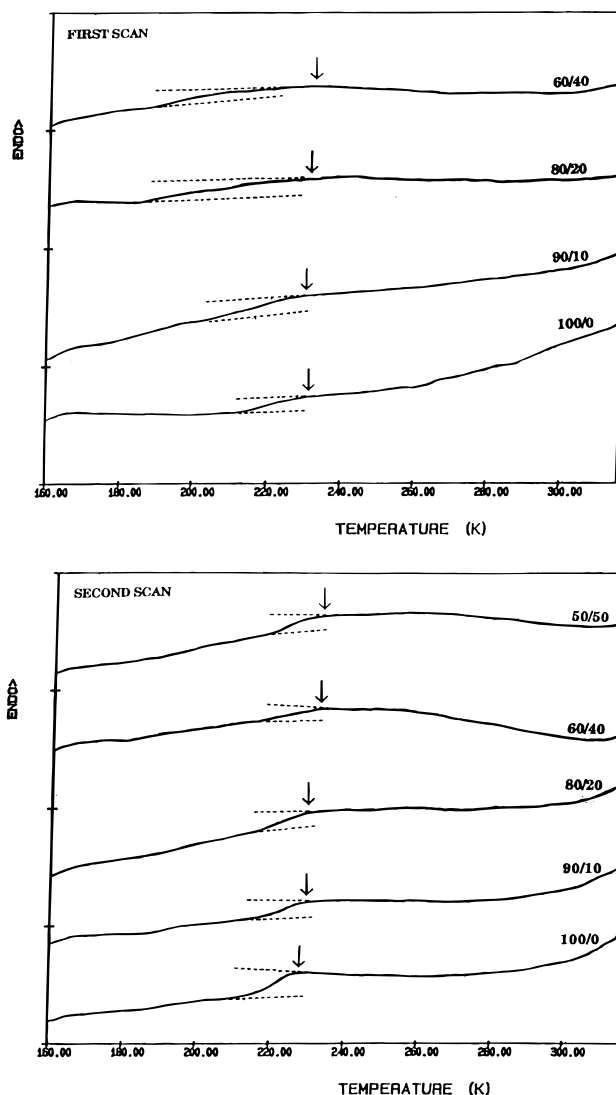


Figure 6. DSC thermograms for PEO/P(MMA-*co*-EMA) samples prepared by the freeze-drying procedure: (a) first scan, (b) second scan. The end of the glass transition zone for each blend is indicated by a vertical arrow.

second runs of the freeze-dried samples. In the first run, it is difficult to locate the glass transition, because the change in the specific heat is very small and the glass transition is broad, but it appears that, at least for the compositions shown in Figure 6a, these blends were phase separated before they were heated in subsequent scans. For samples containing less than 60% PEO, a T_g corresponding to almost pure PEO is not evident in the first scan, possibly due to the small amount of amorphous PEO in these blends. In the second scan (Figure 6b), better-defined T_g 's located around the same temperature as that of the first scan can be seen.

Taking the DSC, DMTA, and ^{13}C NMR results together, it can be concluded that blends with PEO compositions higher than 20 wt % comprise two amorphous phases, one consisting of PEO and P(MMA-*co*-EMA) intimately mixed, and the other consisting of almost pure amorphous PEO. In the literature, similar behavior has been reported for poly(vinylidene fluoride) (PVF₂)/PEMA blends,³⁹ where mixtures containing 80 wt % or more PEMA exhibit single glass transitions which change with composition; while for compositions with low PEMA contents, crystalline regions coexist with two amorphous phases, one comprised of almost pure PVF₂ and the other of a mixture of PVF₂ and

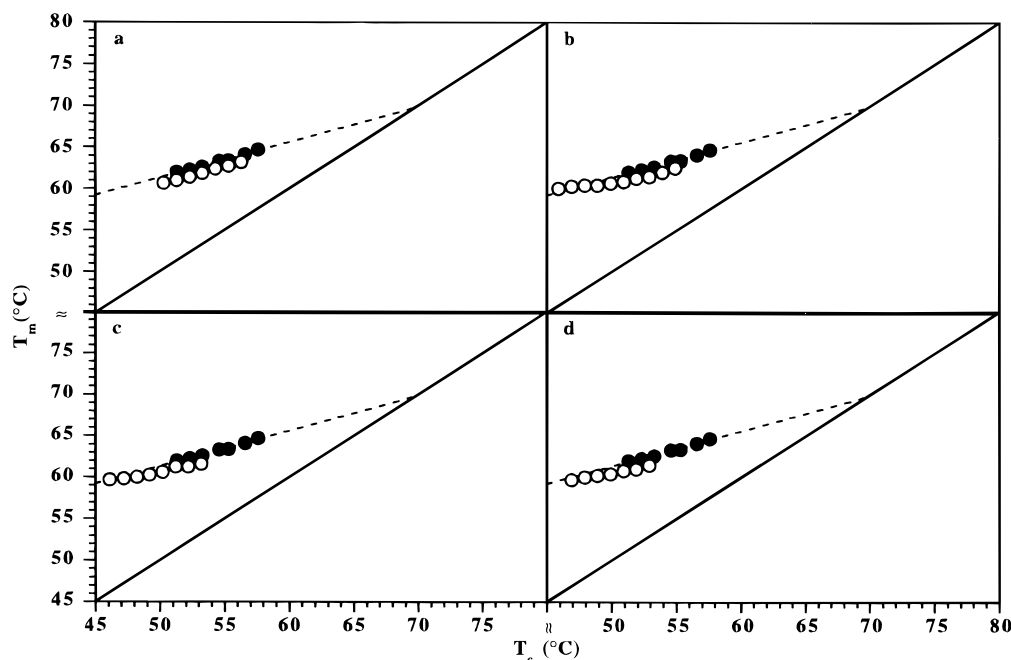


Figure 7. Melting temperature (T_m) from DSC as a function of the crystallization temperature (T_c) for pure PEO (●) and PEO/P(MMA-co-EMA) blends (○): (a) 90/10, (b) 80/20, (c) 60/40, and (d) 50/50.

PEMA. However, this system is reported to be miscible in the molten state as determined by melting point depression measurements. Therefore, the phase behavior of PEO/P(MMA-co-EMA) blends in the molten state ought to be investigated and is presented below.

Melting and Crystallization Behavior. From a thermodynamic point of view, when two polymers are miscible in the molten state, the chemical potential of the crystallizable polymer decreases due to the addition of the second component. This fact causes a reduction in the equilibrium melting temperature of the resulting blend. By contrast, for two totally immiscible polymers, no such decrease of the melting point is expected, at least on exclusively thermodynamic grounds. Since the pioneering work of Nishi and Wang,⁴⁰ the melting point depression has been a useful technique for determining the extent of polymer-polymer miscibility. However, the method is not free from complications,^{17,41,42} and the use of this technique requires previous knowledge of the equilibrium melting temperatures of crystallizable blends, generally in terms of the Hoffman and Weeks procedure.⁴³

Figure 7 shows the melting temperature, T_m , of pure PEO and several PEO/P(MMA-co-EMA) blends as a function of the crystallization temperature, T_c , as determined by DSC for samples obtained by the freeze-drying method. According to the Hoffman and Weeks analysis,⁴³ the intercept of the line corresponding to $T_m = T_c$ with that extrapolated from T_m data gives the equilibrium melting temperature (T_m°) of the polymeric system. For pure PEO, a value of $T_m^\circ = 342.9$ K was obtained. This value agrees with those reported by other authors for this semicrystalline polymer.^{16,17,44} From the plots shown in Figure 7, it is worth mentioning the small decrease in T_m (~ 1 K) obtained at a given T_c as the amount of amorphous copolymer increases. This behavior is contrary to expectation for a homogeneous miscible blend, where the higher the amount of amorphous polymer, the lower the melting temperature of the crystals at a given T_c . As a consequence, and taking into account the uncertainties inherent in the method,^{17,41,42} it would be meaningless to calculate a

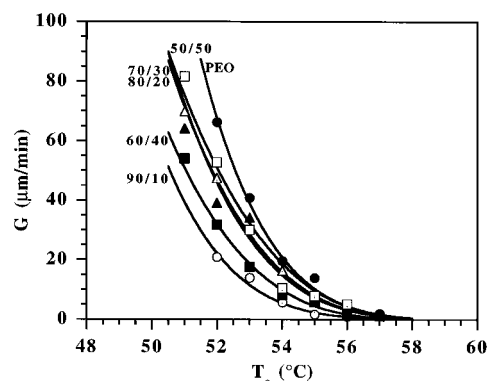


Figure 8. Dependence of the spherulitic growth rate (G) on the crystallization temperature (T_c) for PEO/P(MMA-co-EMA) blends: (●) PEO, (○) 90/10, (▲) 80/20, (△) 70/30, (■) 60/40, and (□) 50/50.

value for the interaction energy density from extrapolated equilibrium melting temperatures of PEO in the blends and to draw any conclusion from it. However, further insight into the miscibility of PEO/P(MMA-co-EMA) blends can be obtained from the crystallization process analysis as we will see below.

Upon addition of a miscible high- T_g amorphous polymer to a crystallizable one, it can be expected that the spherulite growth rate (G) decreases monotonically by increasing the amount of the amorphous component in the blend.^{3,45,46} This is mainly a consequence of the dilution of the crystallizable elements at the growth front and the depression of the segmental mobility due to the higher T_g of the amorphous polymer, among other factors. In terms of the classical nucleation theory,⁴⁷ G is related to a chain mobility parameter (β_g) and the nucleation constant (K_g) by means of the following expression

$$G \propto \beta_g \exp\left(\frac{-K_g}{T_c f \Delta T}\right) \quad (3)$$

where ΔT is the difference between the equilibrium melting temperature T_m° and T_c , and f is a correction

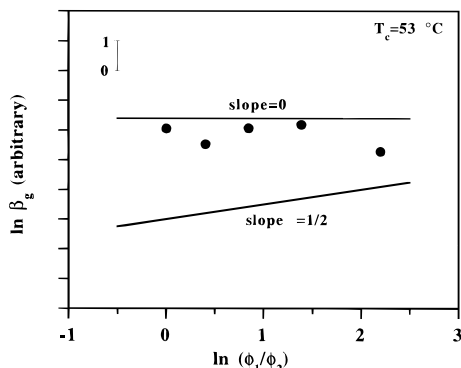


Figure 9. Dependence of the chain mobility parameter (β_g) on the ratio of volume fractions of PEO and P(MMA-*co*-EMA) (ϕ_1/ϕ_2) at $T_c = 53$ °C. The solid lines of slope $1/2$ and 0 are theoretical predictions for miscible (eq 4) and immiscible (eq 5) blends, respectively.

factor given by $2T_c/(T_m^\circ + T_c)$. In the case of a homogeneous blend, it can be shown (see the Appendix) that the chain mobility term^{48,49} follows the scaling behavior given by

$$\ln \beta_g \propto \frac{1}{2} \ln \left(\frac{\phi_1}{\phi_2} \right) + \frac{1}{2} (\ln D_1 + \ln D_2) \quad (4)$$

where ϕ_i and D_i are the volume fraction and the self-diffusion coefficient of component i , respectively. Conversely, in the limiting case of a totally immiscible blend, one can expect

$$\ln \beta_g \propto \ln D_1 \quad (5)$$

Hence, an analysis of both the growth rates and the mobility terms could provide information about the miscibility degree in this kind of polymer blend system.

Spherulite growth rates (G) for neat PEO and PEO/P(MMA-*co*-EMA) blends were obtained from the time variation of the spherulite radii at each crystallization temperature (T_c). Linear growth was observed in both the pure crystalline polymer and in the blends. Figure 8 shows the dependence of G on T_c for several blend compositions. As can be seen, at each T_c there is a certain decrease in G upon addition of P(MMA-*co*-EMA). The growth rate reduction is larger for the blend with 10 wt % of copolymer than for the remaining ones, and no clear systematic trend in the growth rate with blend composition was found. In addition, the range of crystallization temperatures for the blends is roughly the same as for neat PEO. This behavior is usually found for partially miscible systems where minor changes in G and the crystallization range temperatures occur by increasing the amount of the noncrystallizable component.^{50–52}

Referring to chain mobility parameters for PEO/P(MMA-*co*-EMA) blends, they were estimated^{49,53} at several crystallization temperatures by subtracting the secondary nucleation term in eq 3, $\exp(-K_g/T_c f \Delta T)$, from the corresponding values of G . The results for $T_c = 53$ °C are represented in Figure 9. For comparison, we have also included in this figure two lines calculated according to eqs 4 and 5, corresponding to miscible (slope = $1/2$) and totally immiscible (slope = 0) blends, respectively. As can be seen, the values of the chain mobility parameters of PEO/P(MMA-*co*-EMA) blends are similar to those of neat PEO, suggesting a lack of miscibility between components in the melt state, since

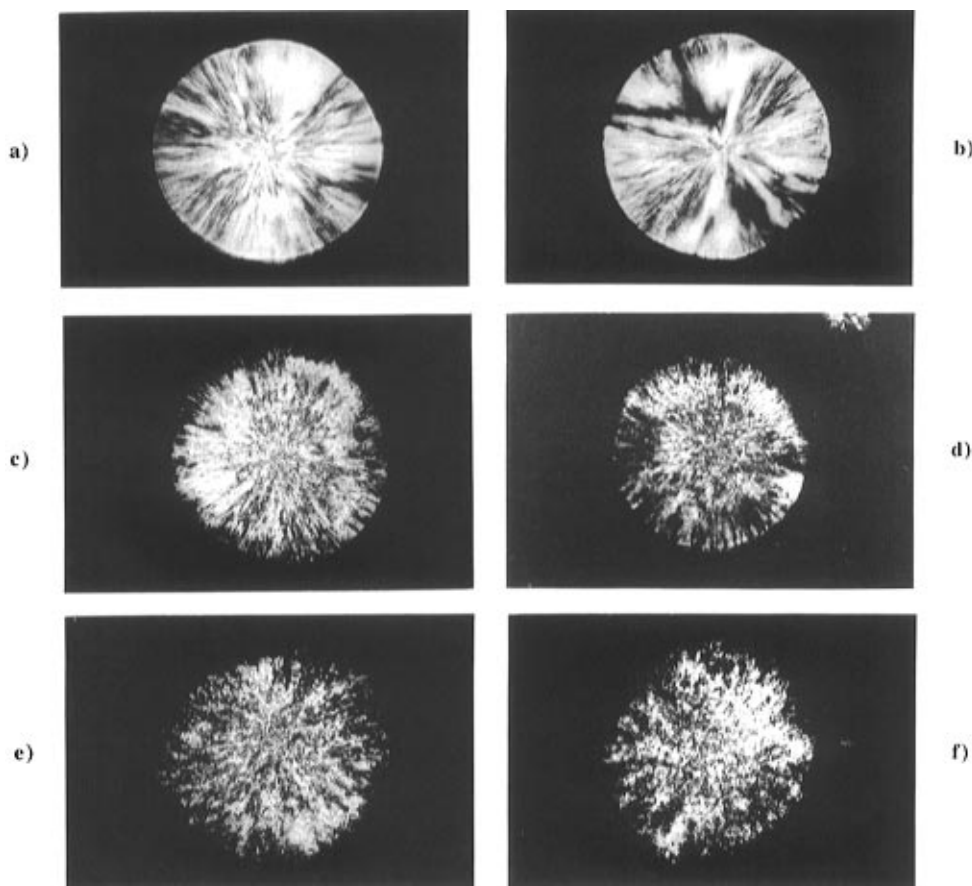


Figure 10. Spherulitic morphology of PEO/P(MMA-*co*-EMA) blends isothermally crystallized at 53 °C: (a) 100/0, (b) 90/10, (c) 80/20, (d) 70/30, (e) 60/40, and (f) 50/50.

no clear influence of the copolymer in the diffusion process near the growth front is apparent. However, microscopic observations (Figure 10) for samples containing less than 30% of copolymer did not show the presence of segregated domains exceeding the resolution power of thermo-optical analysis. When the amount of copolymer in the blend increases, the morphology of the spherulites is seriously affected, leading progressively to a granular morphology.

From the above results, we can reasonably conclude that the melting and crystallization behavior of this system is, in fact, more close to that of a heterogeneous system than that of a homogeneous one.

Conclusions

The following conclusions can be drawn from this study.

(1) Miscibility is predicted for blends of PEO and P(MMA-co-EMA) copolymers with high methyl methacrylate content from a simple binary interaction model using low molecular weight liquids closely related to the chemical structure of the polymer repeat units. Blends involving a copolymer with a 60 wt % MMA content are predicted to be immiscible or, at least, at the margin of miscibility.

(2) Lack of miscibility is found from complementary DSC and DMTA data for the glass transition behavior of binary blends of PEO and P(MMA-co-EMA) with 60 wt % MMA, in good agreement with the above prediction. Two phases are present in this system, across a broad composition range, a PEO-rich phase and a copolymer-rich phase, the latter with a certain degree of mixing between PEO and P(MMA-co-EMA) components as determined by ^{13}C NMR measurements, the former being an almost pure amorphous PEO phase, as determined by DSC and DMTA.

(3) In addition, the melting and crystallization behavior of the blends show no clear evidence of miscibility in the melt state. Neither the Hoffman-Weeks analysis nor a new analysis proposed in this paper concerning the composition dependence of the mobility parameters of the classical growth rate expression suggest miscibility in the system analyzed.

Acknowledgment. We are pleased to acknowledge financial support of this work by the Diputación Foral de Gipuzkoa (Programa Marco de Apoyo a la PYME 1994).

Appendix

For crystallization conditions such that many deposited stems are growing simultaneously at different points on the substrate, it has been proposed by Saito et al.⁴⁹ that β_g can be formulated as

$$\beta_g \propto \phi_1^{1/2} (D_1 D_M)^{1/2} \quad (1A)$$

where ϕ_1 and D_1 are the volume fraction and the self-diffusion coefficient of the crystalline polymer, respectively, and D_M is the mutual diffusion coefficient of the blend. According to Brochard et al.⁴⁸ D_M can also be related to the self-diffusion coefficients of the blend components (D_i) by means of the following relationship:

$$D_M \propto \frac{1}{\left(\frac{\phi_1}{D_1}\right) + \left(\frac{\phi_2}{D_2}\right)} \quad (2A)$$

Since, at the crystallization temperature, the self-diffusion coefficient of a high- T_g amorphous polymer (D_2) may be several orders of magnitude lower than that of the crystallizable component (D_1), eq 1A can be rewritten, to a first approximation, as

$$\beta_g \propto \left(\frac{\phi_1}{\phi_2}\right)^{1/2} (D_1 D_2)^{1/2} \quad (3A)$$

On the other hand, for a totally immiscible blend it can reasonably be assumed that $\phi_1 = 1$ and $D_M = D_1$ at the growing front, and thus eq 1A becomes

$$\beta_g \propto D_1 \quad (4A)$$

References and Notes

- (1) Coleman, M. M.; Graf, J. F.; Painter, P. C. *Specific Interactions and the Miscibility of Polymer Blends*; Technomic Publishing Co.: Lancaster PA, 1991.
- (2) Olabisi, O.; Robeson, L. M.; Shaw, M. T. *Polymer-Polymer Miscibility*; Academic Press: New York, 1979.
- (3) Martuscelli, F.; Palumbo, R.; Kryszewski, M. *Polymer blends: Processing Morphology and Properties*; Plenum Press: New York, 1981.
- (4) Utracki, L. A. *Polymer Alloys and Blends*; Hanser Publishers: New York, 1989.
- (5) Kambour, R. P.; Bendler, J. T.; Bopp, R. C. *Macromolecules* **1983**, *16*, 753.
- (6) ten Brinke, G.; Karasz, F. E.; Macknight, W. J. *Macromolecules* **1983**, *16*, 1827.
- (7) Paul, D. R.; Barlow, J. W. *Polymer* **1984**, *25*, 487.
- (8) Nishimoto, M.; Keskkula, H.; Paul, D. R. *Macromolecules* **1990**, *23*, 3633.
- (9) Jo, W. H.; Lee, S. C. *Macromolecules* **1990**, *23*, 2261.
- (10) Huh, W.; Karasz, F. E. *Macromolecules* **1992**, *25*, 1057.
- (11) Walsh, D. J.; Cheng, G. L. *Polymer* **1984**, *25*, 499.
- (12) Barlow, J. W.; Paul, D. R. *Polym. Eng. Sci.* **1987**, *27*, 1482.
- (13) Landry, C. J. T.; Teegarden, D. M. *Macromolecules* **1991**, *24*, 4310.
- (14) Pedrosa, P.; Pomposo, J. A.; Calahorra, E.; Cortazar, M. *Macromolecules* **1994**, *27*, 102.
- (15) Cortazar, M.; Calahorra, E.; Guzman, G. M. *Eur. Polym. J.* **1981**, *19*, 1925.
- (16) Martuscelli, E.; Pracella, M.; Yue, W. P. *Polymer* **1984**, *25*, 1097.
- (17) Alfonso, G. C.; Russell, T. P. *Macromolecules* **1986**, *19*, 1143.
- (18) Liberman, S. A.; Gomes, A. S.; Macchi, E. M. *J. Polym. Sci.* **1984**, *22*, 2809.
- (19) Ito, H.; Russel, T. P.; Wignall, G. D. *Macromolecules* **1987**, *20*, 2213.
- (20) Cimmino, S.; Martuscelli, E.; Silvestre, C. *Makromol. Chem., Makromol. Symp.* **1988**, *16*, 147.
- (21) Cimmino, S.; Martuscelli, E.; Silvestre, C.; Canetti, M.; Lalla, C.; Selves, A. *J. Polym. Sci. Part B* **1989**, *27*, 1781.
- (22) Kewi, T. K.; Frish, H. L.; Radigan, W.; Vogel, S. *Macromolecules* **1977**, *10*, 157.
- (23) Goh, S. H.; Siow, K. S. *Thermochim. Acta* **1986**, *105*, 191.
- (24) Pomposo, J. A.; Calahorra, E.; Eguiazabal, I.; Cortazar, M. *Macromolecules* **1993**, *26*, 2104.
- (25) J. I. Kroschwitz *Polymer Characterization and Analysis*; John Wiley and Sons: New York, 1990.
- (26) Min, K. E.; Chiou, J. S.; Barlow, J. W.; Paul, D. R. *Polymer* **1987**, *28*, 1721.
- (27) de Juana, R.; Hernandez, R.; Peña, J. J.; Santamaría, A.; Cortazar, M. *Macromolecules* **1994**, *27*, 6980.
- (28) Murayama, T. *Dynamical Mechanical Analysis of Polymeric Materials*; Elsevier: New York, 1978.
- (29) Landry, C. J. T.; Henrichs, M. P. *Macromolecules* **1989**, *22*, 2157.
- (30) Diaz-Calleja, R.; Ribes-Greus, A.; Gomez-Ribelles, J. L. *Polymer* **1989**, *30*, 1433.
- (31) Dickinson, L. C.; Yang, H.; Chu, C. W.; Stein, R. S.; Chien, J. C. W. *Macromolecules* **1987**, *20*, 1757.
- (32) Koenig, J. L. *Spectroscopy of Polymers*; American Chemical Society: Washington, DC, 1992.
- (33) Stejskal, E. O.; Schaefer, J.; Sefcik, M. D.; McKay, R. A. *Macromolecules* **1981**, *14*, 275.
- (34) Henrichs, P. M.; Tribone, J.; Massa, D. J.; Hewitt, J. *Macromolecules* **1988**, *21*, 1282.

- (35) Sofue, S.; Tamura, N. *J. Appl. Polym. Sci.: Appl. Polym. Symp.* **1993**, 52, 261.
- (36) Hung, C. C.; Carson, W. G.; Bohan, S. P. *J. Polym. Sci.: Polym. Phys. Ed.* **1994**, 32, 141.
- (37) Tekely, P.; Lauprêtre, F.; Monnerie, L. *Polymer* **1985**, 26, 1081.
- (38) Marco, C.; Fatou, J. G.; Gómez, M. A.; Tanaka, H.; Tonelli, A. E. *Macromolecules* **1990**, 23, 2183.
- (39) Kwei, T. K.; Patterson, G. D.; Wang, T. T. *Macromolecules* **1976**, 9, 780.
- (40) Nishi, T.; Wang, T. T. *Macromolecules* **1975**, 8, 909.
- (41) Rim, P. B.; Runt, J. P. *Macromolecules* **1984**, 17, 1520.
- (42) Alamo, R. G.; Viers, B. D.; Mandelkern, L. *Macromolecules* **1995**, 28, 3205.
- (43) Hoffman, J. D.; Weeks, J. J. *Res. Natl. Bur. Stand.* **1962**, 66, 13.
- (44) Pedrosa, P.; Pomposo, J. A.; Calahorra, E.; Cortazar, M. *Polymer* **1995**, 36, 3889.
- (45) De Juana, R.; Cortazar, M. M. *Macromolecules* **1993**, 26, 1170.
- (46) Ong, C. J.; Price, F. P. *J. Polym. Sci. Polym. Symp. Ed.* **1978**, 63, 59.
- (47) Hoffman, J. D.; Davis, G. T.; Lauritzen, J. I., Jr. *Treatise on Solid-State Chemistry*; Hannay, N. B., Ed.; Plenum Press: New York, 1976.
- (48) Brochard, F.; Jouffroy, J.; Levinson, P. *Macromolecules* **1988**, 16, 1683.
- (49) Saito, H.; Okada, T.; Toshihiko, H.; Inoue, T. *Macromolecules* **1991**, 24, 4446.
- (50) Martuscelli, E.; Silvestre, C.; Bianchi, L. *Polymer* **1983**, 24, 1458.
- (51) Cimmino, S.; Martuscelli, E.; Silvestre, C.; Cecere, A.; Fontelos, M. *Polymer* **1993**, 34, 1207.
- (52) Bartzak, Z.; Galeski, A.; Martuscelli, E. *Polym. Eng. Sci.* **1984**, 24, 1155.
- (53) Okada, T.; Saito, H.; Inoue, T. *Polymer* **1994**, 35, 5699.

MA9518969